Quartz resonator based low-energy ionizing radiation detection

J.-M Friedt [2], C. Mavon [1], S. Ballandras [2], V. Blondeau-Patissier [2], M. Fromm [1]

[1] Laboratoire de Microanalyses Nucléaires A. Chambaudet, UMR CEA E4, Université de Franche-Comté, 16 route de Gray, 25030 Besançon FRANCE

[2] Institut FEMTO-ST, Département LPMO, 32 avenue de l'Observatoire, 25044 Besançon FRANCE

Our work aims at the development of a wireless, remote sensing method for quantitatively measuring radiation doses. We have selected high-frequency (several 100 MHz to 1 GHz) quartz crystal resonators as probes of the ionizing radiation field. We here focus on the effects of low energy X ray and electron beams on these sensors.

As opposed to classical work concerned with eliminating the disturbances induced by radiations, we here attempt to characterize the response of the resonators as a function of dose and radiation energy in order to be able to use the frequency signal as a remotely interrogated radiation probe.

We present results of bulk acoustic wave resonators, surface acoustic wave resonators and surface acoustic wave delay lines under X-rays and electrons irradiation: we interpret all observed signals (frequency or phase shift during electron irradiation) as thermal effects. Hence, surface acoustic wave resonators can make suitable calorimeters, compatible with wireless interrogation, and high sensitivity if a quartz cut with high temperature sensitivity (*Z*-cut) is used.

1   Introduction

Quartz-crystal resonators are suitable for low-power integrated or remotely interrogated sensors [1]. While thickness shear resonators and surface acoustic wave sensors are widely used for mass (quartz crystal microbalance), gas species, pressure and acceleration sensing, we are not aware of their use for radiation detection. The need for small sensors requiring little or no power able to detect photons (X and gamma rays) in the 1-10 000 keV range exists, particularly in medical and environment monitoring applications.

It is now well known that in high energy ionization processes, most of the deposited energy is carried by secondary electrons whose mean energy is low (as defined in LEED[1]: 20-500 eV) in the first generation and very low (<20 eV) in the next generations [2]. These processes are also accompanied by a soft X-rays component, particularly in biological media or low Z materials (electronics). We wish here to assess the influence of low-energy ionizing radiations on the resonance frequency of Bulk Acoustic Wave (BAW) and Surface Acoustic Wave (SAW) resonators.

2   Soft X-rays and low-energy electrons generation

Thanks to a cold-cathode X-rays generating instrument (Fig. 1) [3] with tunable Bremsstrahlung energy spectrum in the 1 to 12 kV range, we monitor the frequency response in an oscillator configuration of commercial quartz BAW resonators as well as STW-SAW [2] sensors to external irradiation. The ionization radiation produced is either soft X rays in the 1-10 keV range in vacuum and in air produced at a rate of about $10^{-3} - 10^{-1}$ Gy/s, or electrons in the 1-10 keV range in vacuum. The spectra of the X-rays generated by the impact of accelerated electrons on a thin (11 or 20 μm thick *Al* foil) has been measured using an Amptek XR100-CR solid state X-rays detector and shown to result in a bremsstrahlung background combined with the strong absorption by the foil of the photons generated in the lower energy part of the spectrum. The resulting energy-spectrum displays a broad peak centered close to the acceleration voltage of the incoming electrons as shown in Fig. 1 (inset).

---

[1]Low Energy Electron Diffraction

[2]Surface Transverse Acoustic Waves (STW) are shear waves propagating on a periodic grating patterned on the piezoelectric substrate.
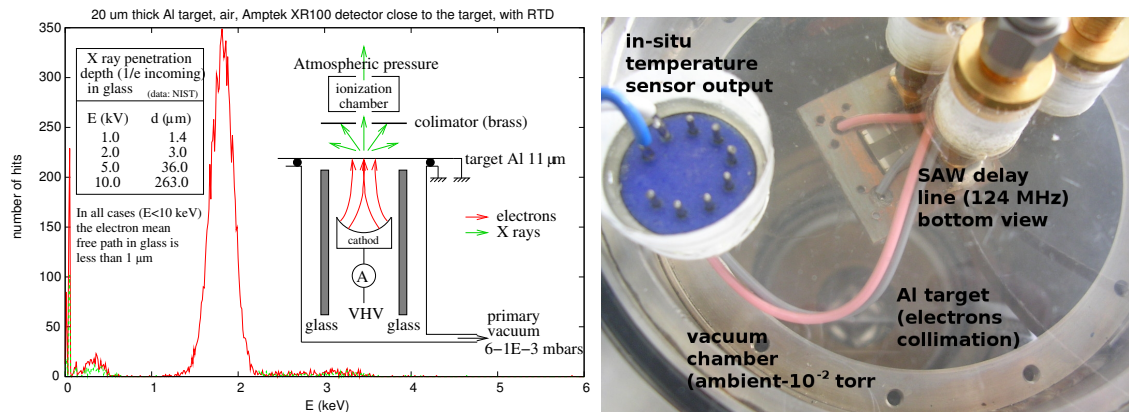
Figure 1: Left: schematic of the cold-cathode X-rays generator and measured X-rays spectrum: the peak is the result of absorption of the low energy X rays by the Al target and air, and the upper limit is defined by the energy of the incoming electrons. Right: picture of the experimental setup displaying the SAW delay line exposed to the electron beam in a vacuum chamber.

3   Calibration of the X-rays KERMA

In order to calibrate the complex relationship between the gas pressure in the plasma-filled cold cathode part of the X-rays generator in which the electrons are accelerated, the electron acceleration voltage and the electron current, we have built an ionizing gas chamber [4] for converting this set of parameters (pressure, voltage, current) to a quantitative estimate of the deposited dose. Thanks to the low energies of interest here, the mean free path of the electrons generated by the interaction of the incoming X-rays with the molecules in air is at most 1.2 mm for incoming radiations with maximum energy 10 keV. We have thus selected to build a chamber with an interaction volume of $1 \times 1 \times 1$ cm^3 and a total volume with homogeneous electric field (15 kV/m) of $27 \times 27 \times 27$ mm^3. Some of the calibration curves are presented in Fig. 2, leading to an estimated KERMA of 3×10^{-3} Gy/s.

4   Effects of ionizing radiations on quartz resonators

We have introduced three types of quartz-resonators under the soft X-rays beam: 12 MHz BAW resonators, STW-SAW resonators included in a oscillator circuit working at 505 MHz, and Love-mode SAW delay lines working around 125 μm made of 2.2 μm thick PECVD-deposited SiO_2 on interdigitated transducers pattered to generate 40 μm-wavelength surface acoustic waves. Both resonators were included in an oscillation loop (shielded from the ionizing radiation beam by a 1.6 mm-thick FR4 epoxy printed circuit board and a sealed 20 mm-thick PMMA window) and the frequencies of a reference oscillator and a probe oscillator were monitored during irradiation. The stability of the resonators were respectively in the range of 1 Hz over the duration of the experiment (10 minutes) for the 12 MHz oscillator, and 100 Hz for the 505 MHz oscillator. In all experiments the amplifier and phase shifter (amplifier electronics) were shielded from the radiations and only the quartz resonator was submitted to the irradiation beams. The delay line was probed at a fixed frequency (in the 124-125 MHz range) during a given experiment, the electric signal being provided by an AD9850 DDS and amplitude/phase information being extracted by an AD8302 I/Q circuit, leading to a fully embedded instrument.

In all cases (12 and 505 MHz oscillators, 125 MHz delay line) X-rays irradiation with a beam whose energy ranged from 1.5 ($K_\alpha(Al)$ line) to 5 keV leads to no significant ($\Delta f/f < 0.2$ ppm) change of the oscillators frequencies.

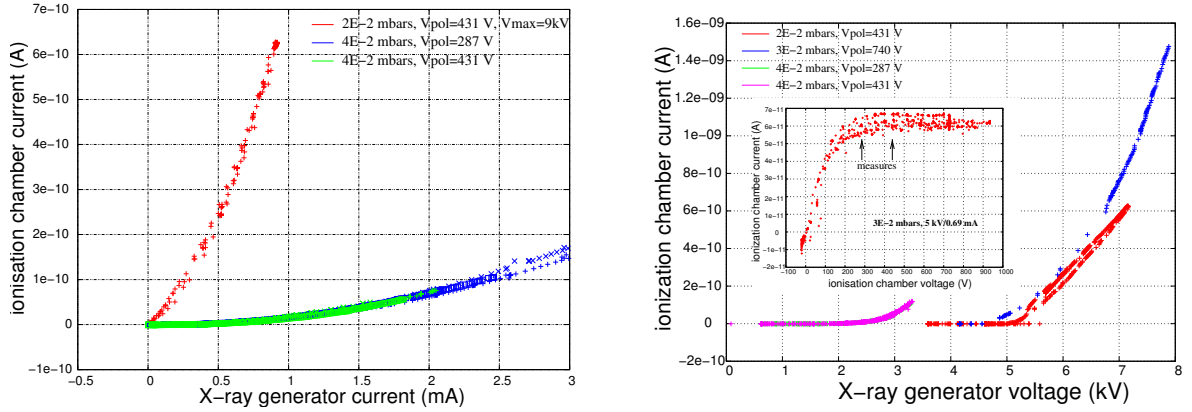On the opposite, both oscillators and the delay line submitted to the direct irradiation by

Figure 2: Left: current output from the ionization chamber as a function of cathode current. The higher the cathode current, the higher the KERMA measured by the ionization chamber. At lower pressure in the cathode chamber, a higher voltage is needed to reach a given cathode current (the lower the pressure in the cathode chamber, the higher the impedance of the plasma formed between the cathode and the foil target) and hence a higher KERMA is measured since the absorption cross section of the target foil decreases with increasing generated X-rays energy. Right: current output from the ionization chamber as a function of cathode polarization voltage. The lower the pressure in the cathode chamber, the lower the cathode current and hence the lower the KERMA for a given cathode voltage, hence the complementarity of this chart with the one shown on the left part of this figure. Inset: current output from the ionization chamber as a function of the ionization chamber polarization voltage. We work at the saturation level (> 270 V) where the output current of the ionization chamber is independent of the polarization voltage and only depends of the incoming ionizing radiation dose.
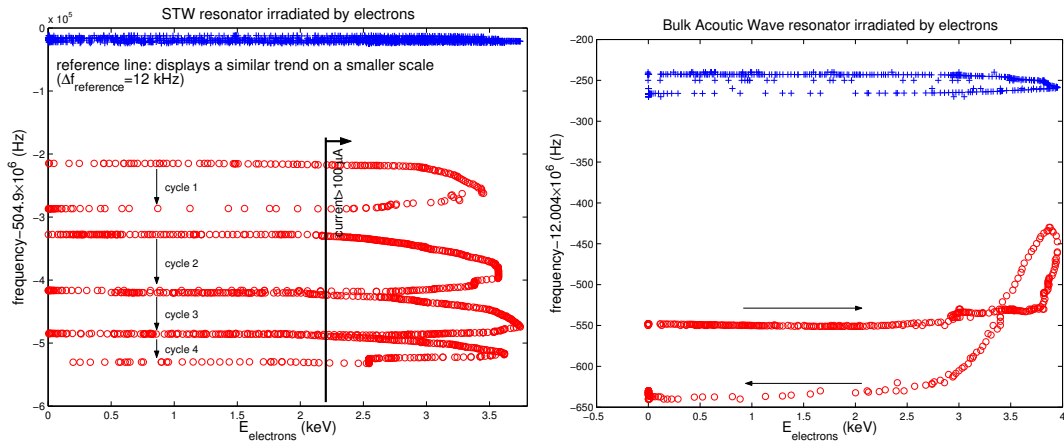

Figure 3: Left: experimental frequency measurement of two STW delay lines oscillating around 504.7 MHz. One delay line acting as a reference (+ sign) was shielded from incoming radiations, while the measurement line (circles) was subject to direct irradiation by an electron beam of varying energy as indicated by the abscissa. The frequency of the measurement line is observed to decrease during each successive experiment, each experiment occurring during about 5 minutes and separated by a few minutes. Right: same experiment performed with 12.0 MHz bulk acoustic wave resonators.

accelerated electrons displayed significant frequency shifts with respect to the reference oscillator (Fig. 3). We observe large frequency decreases during electron irradiation. Possible causes are

heating of the resonator [5], charge accumulation on the insulating quartz surface, the migration of impurities in the quartz lattice [6, 7] or growth of defects [8]. The reproducibility of the response (reversible and permanent effects [9]) and the dependence upon each possible cause as a function of the grade of the quartz (natural, synthetic [5, 10]) is examined.

In order to clarify the origin of the detected frequency change we included in the delay line design a thin metallic strip used as thermistor. The 180 nm thick, 10 μm wide metallic strip displays at room temperature a resistance of 2280 Ω. We calibrated the temperature sensitivity of this thermistor as being around 3.5 Ω/K. This value, far from the $\Delta R/R = 4300$ ppm/K resistivity thermal coefficient of aluminum, might be due to the thin film deposition process.
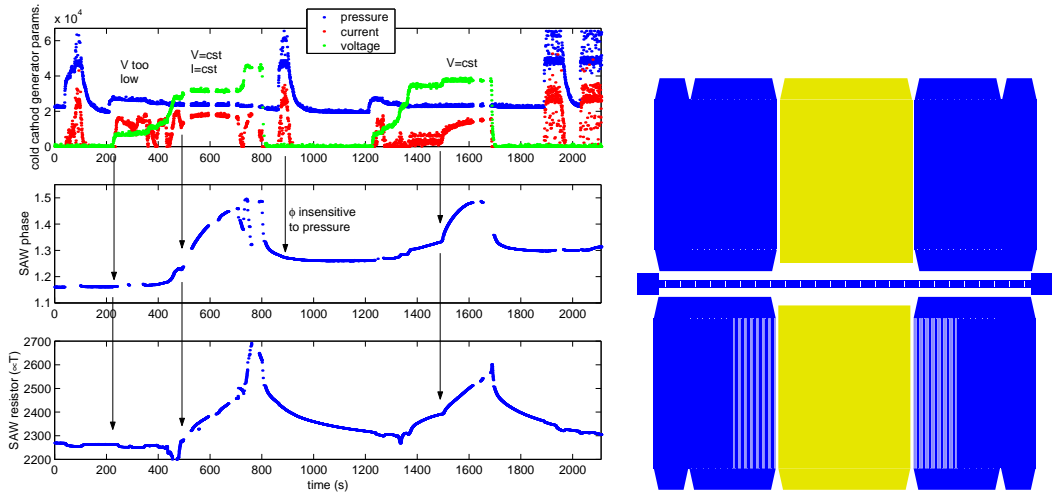

Figure 4: Left: typical experiment of an irradiation by electrons of a surface acoustic wave delay line. The top graph displays the time-evolution of the parameters of the electron generator: the chamber pressure, the cathode current and voltage as controlled by the operator (two of these parameters are tuned by the operator and the third results from the properties of the plasma formed in the vacuum chamber). Middle: evolution of the phase at fixed frequency. Bottom: evolution of the resistance of the thermistor patterned on the substrate. Right: design of the surface acoustic wave Love-mode delay line including a reference and measurement lines (blue – acoustic wavelength of 40 μm) patterned on a common substrate (AT-cut quartz) as well as the thermistor in between for in-situ temperature measurement. The central yellow area between the transducers is a metal (gold) coated area for collecting electrons and thus avoiding charge buildup as well as allowing a direct measurement of the current hitting the sensing area. This whole sensor fits in a 1×1 cm^2 square.

Fig. 4 displays the result of an experiment in which all electron generator parameters were recorded (acceleration voltage, anode current, chamber pressure) as well as delay line phase at a fixed frequency of 125.3560 MHz. We observe that at lower acceleration voltage around 1.7 kV (left-most arrow on fig. 4) the delay line is hardly affected, probably because all electrons are slowed down before reaching the sensor located 20 cm from the target. On the other hand, once a threshold acceleration voltage of around 6 kV (second arrow from left on fig. 4), both acoustic delay line phase and thermistor resistance sharply increase, consistent with a mostly temperature-related effect. We observe that pressure (from 3×10^{-2} torr as shown by a value of 25000 on the top most graph of fig. 4, to ambient when the value read is around 65000) does not affect the acoustic wave delay line response as seen in the area around the third arrow from left of fig. 4. The fourth arrow reproduces the result of increasing temperature and phase shift once the threshold voltage is reached. In this last case the thermistor resistance increased by 320 Ω, *i.e.* a substrate temperature increase by 90 to 100 K.

This conclusion – that the frequency shift of resonators is consistent with temperature drift effects – is supported by STW-SAW and BAW resonators which displayed sensitivity to electron irradiation in the 1 to 5 keV range but no evidence of effects by X-rays irradiation in the same energy range has been observed. From this observation two conclusions can be drawn:

- from a calculation of the energy deposited by the electrons in the quartz matrix we can estimate the detection threshold of this sensor to X-rays. Indeed, our current EDX-like X-rays production method is highly inefficient and the X-rays doses might be insufficient to trigger a response from such a crude sensor

- a suitable quartz cut might be chosen – Z cut – for *maximum* temperature coefficient of the resonator or delay line fabrication. Hence, rather than focusing on some unidentified effect of radiations on quartz, we focus on the realization of a sensitive calorimeter compatible with wireless remote sensing.

5 Perspectives

Improvements of the current measurement setup include the use of a wireless interrogation setup of the resonator as required for our final application, but most important the identification of the material parameter leading to the *largest* and most *reproducible* response to irradiations as required for sensing applications. Assuming we can identify the whole sensor response as resulting from thermal effects (as will be verified following accurate thermal characterization of the resonators and delay lines), a Z-cut based quartz sensor seems most promising in providing high sensitivity due to its large temperature coefficient.

Acknowledgment

References

[1] F. Seifert, A. Pohl, R. Steindl, L. Reindl, M.J. Vellekoop, and B. Jakoby, *Wirelessly interrogable acoustic sensors*, Joint Meeting EFTF-IEEE IFCS (1999), pp.1013-1018

[2] S. Uehara, H. Nikjoo, and D.T. Goodhead, *Comparison and assessment of electron cross sections for Monte Carlo track structure codes*, Radiat. Res. **152** (1999), pp.202-213

[3] M. Hoshi, D.T. Goodhead, D.J. Brenner, D.A. Bance, J.J. Chmielewski, M.A. Paciotti, and J.N. Bradbury JN, *Dosimetry comparison and characterisation of an Al K ultrasoft x-ray beam from an MRC cold-cathode source*, Phys. Med. Biol. **30** (1985), pp.1029-1041

[4] G.F. Knoll, *Radiation detection and measurement*, John Wiley & Sons (2000) 3rd Ed., p.134

[5] H.J. Benedikter, J.H. Sherman, and R.D. Gillepsie, *The effect of gamma irradiation on the temperature-frequency characteristics of AT-cut quartz*, 28th Annual Frequency Control Symposium (1974), pp.143-149

[6] H. Bahadur, and R. Parshad, *Simple experimental method for demonstrating transient frequency shifts in X- and gamma-irradiated quartz crystals*, Rev. Sci. Instrum. **51** (10) (Oct. 1980), pp.1420-1421

[7] L.E. Halliburton, N. Koumvakalis, M.E. Markes, and J.J. Martin, *Radiation effects in crystalline SiO_2: the role of aluminum*, J. Appl. Phys **52** (5) (May 1981), pp.3565-3574

[8] M.A. Stevens-Kalceff, M.R. Phillips, and A.R. Moon, *Electron irradiation-induced changes in the surface topography of silicon dioxide*, J. Appl. Phys. **80** (8) (Oct. 1996), pp.4308-4314

[9] A. Kahan, F.K. Euler, H.G. Lipson, C.Y. Chen, and L.E. Halliburton, *Radiation effects in vacuum-swept quartz*, 41st Annual Frequency Control Symposium (1987), pp.216-222

[10] J.C. King, and H.H. Sander, *Rapid annealing of frequency change in high frequency crystal resonators following pulsed X-irradiation at room temperature*, 27th Annual Frequency Control Symposium (1973), pp.113-119